International Journal of
INTELLIGENT SYSTEMS AND APPLICATIONS IN ENGINEERING
ISSN:2147-6799 www.ijisae.org Original Research Paper

Intelligent Controller for Mitigating Power Quality Issues in Hybrid Fuzzy Based Microgrid Applications

Naresh Kumar[1,*], Anwar Shahzad Siddiqui[2], Rajveer Singh[3]

Submitted: 13/11/2022 **Revised**: 22/01/2023 **Accepted**: 10/02/2023

Abstract: An intelligent controller for the enhancement of power quality of a hybrid energy source based microgrid that encompasses Wind-PV-Battery is discussed in this work. Global warming coupled with climate change, is one of the most critical crisis that the world faces today. Transitioning to renewable energy sources for power generation, like solar and wind, minimises carbon emissions and aids in tackling climate change. For ensuring a stable and uninterrupted supply of power, a Battery Energy Storage System (BESS) is added to microgrid in order to overcome the intermittency and instability associated with both Wind Energy Conversion System and PV. The PV output voltage is transformed to anticipated level by employing Interleaved Boost Converter (IBC) with excellent efficiency and voltage gain. Conversion efficiency of PV system is heightened by the application of CFLC based MPPT technique, which facilitates a transference of maximum power grid. The AC output from Doubly Fed Induction Generator (DFIG) built WECS is converted to DC using a PWM rectifier controlled by Proportional Integral (PI) controller. The charging and discharging of the battery are effectively carried out using a Battery converter with bidirectional power flow capability. The control of the Battery converter for managing State of Charge (SOC) of battery is accomplished with an aid of PI controller. Conversion of stable DC to AC voltage is established using 3φ Voltage Source Inverter (VSI) and minimization of harmonics is achieved using LC filter. The grid voltage synchronization is also performed successfully utilizing PI controller. The proposed hybrid microgrid is simulated by MATLAB and the effective performance of suggested control approach in maintaining the power quality and stability of the microgrid is verified.

Keywords: *PV system, DFIG based WECS, PI controller, Interleaved Boost converter, CFLC, Battery converter, Battery*

1. Introduction

Electrical energy is the driving force behind the propulsion of the modern world and all sectors are heavily reliant on it for their effective functioning. Nuclear energy and fossil fuels provide for nearly 80% of total electrical energy generated, which has resulted in the threat of global warming due to the increase in release of greenhouse gases. The nuclear power plants do not produce carbon emissions, but on the downside, they generate radioactive waste, which poses significant transportation, processing and storage challenges. Moreover, the concerns that exists around the availability and pricing of fossil fuels has also propelled the need for development of cleaner and sustainable energy generation system. As a result, there has been a large-scale influx of renewable sources of energy such as solar and wind energy for power generation in recent years. Despite being the most appropriate and effective method for providing sustainable power generation, renewable energy sources have the shortcoming of intermittency. Hence, energy storage devices are integrated with the wind and solar energy for heightening the reliability and sustainability of the hybrid energy system [1-4]. The stable and smooth working of hybrid power system is ensured with the assistance of efficient control techniques.

In case of PV, regular phenomena such as shading, cloud formation, temperature, and meteorological conditions influences output power of solar; this is cracked by engaging DC-DC converter in concurrence with MPPT technique to extract maximal available power from solar panels. A primary function DC-DC converter is to regulate PV module voltage for enabling transference of maximum power to the load or grid, regardless of changes in operating conditions [5, 6]. The boost converter has a simple construction and are typically employed in PV system for voltage boosting; however, owing to switching losses, conduction losses and voltage spike over switch, are

[1] *Assistant Professor, University Polytechnic, F/o Engineering and Technology, Jamia Millia Islamia, Central University, New Delhi*
[1] *Professor, Department of Electrical Engineering, Jamia Millia Islamia (Central University), New Delhi, assiddiqui@jmi.ac.in*
[1] *Assistant Professor, Department of Electrical Engineering, F/o Engineering and Technology, Jamia Millia Islamia, Central University, New Delhi-110025, rsingh@jmi.ac.in*
[*] *Corresponding Author Email: nareshknk3082@gmail.com*

inapplicable for high gain set-ups [7, 8]. The buck-boost converters require the assistance of huge decoupling capacitor for carrying out effective MPPT operation since its input current is not continuous. The Cuk converter and SEPIC converter, unlike the buck-boost converter have continuous input current but their MPPT performance is poor due to the existence of large amount of current ripples [9, 10]. For enhancing the conversion efficiency of the PV system, it is considered essential to adopt a suitable MPPT method. The Perturb and Observation (P&O) is a frequently utilized simple conventional MPPT approach. When there is a significant increase in incoming irradiance, the P&O is not capable of maintaining its tracking direction and its operating point is always varying resulting in considerable amount of loss in energy. The conventional approaches like Incremental Conductance and Hill Climbing are not suitable for PV systems, since they are not efficient in detecting Maximum Power Point (MPP) under partial shading condition. In addition, these conventional MPPT techniques lack the capability of self-learning and they have slow transient response and high steady state error. So artificial intelligence based MPPT approaches are developed for overcoming the limitations of conventional approaches. To enable PV panels to generate maximum power, Artificial Neural Network (ANN) adjusts itself to the characteristics of PV system by gathering several data such as temperature, irradiance, input current, and input voltage. The Fuzzy Logic Controller (FLC) is simple, efficient and most widely used MPPT method with excellent dynamic performance. Both soft computing MPPT techniques are extremely effective, but they have shortcomings owing to their complex structure and reduced tracking speed [11-13].

The wind energy is another widely available renewable source of energy, which is clean and emission free with huge potential. The aerodynamics of wind turbines, power electronic conversions, mechanical processes, electric generators, connectivity with power systems, and controlling concept have all seen significant advancements in recent decades. Among different types of WECS technology, turbine equipped with DFIG is widely used because it provides advantages of enhanced active and reactive power control, better power capture capability, lower converter ratings, minimized mechanical stress, enhanced power quality in addition to wide speed operational range [14, 15]. With the increased penetration of variable renewable sources of energy, dynamic balance between electricity generation and load is required to be maintained always. So an Energy Storage System (ESS), which enhances the resiliency, flexibility, efficiency and stability of the electric grid is added to significantly enhance the intermittency in power generation [16].

This study proposes a hybrid Wind-PV-Battery microgrid. Maximum power from panel is extracted and supplied to grid using CFLC based MPPT and IBC. A PI controller is engagaed to stabilise output from DFIG-based WECS. Surplus power from PV and WECS is stored in BESS, which serves as a backup power source for tacking the intermittency of renewable sources of energy. A battery converter is used to connect the battery to the microgrid, and a PI controller is used to manage the battery's state of charge. The control of 3φ VSI with the PI controller achieves efficient grid synchronisation.

2. Proposed System Description

PV system provide electricity during the day, while WECS provides electricity throughout the day and night, so both PV and WECS help to mediate power imbalances. An output of solar photovoltaic system is non-linear due to variation in solar irradiance and weather intermittency. As a result, output of photovoltaic system is regulated and maximized with applications of IBC. For extracting maximum available power from PV panels, the operating point is controlled by cascaded fuzzy MPPT technique. An output voltage V_{PV} of and output current I_{PV} of PV panel are set as input to cascaded Fuzzy MPPT controller for estimation of operating point V_{mpp}. PWM generator produces PWM pulses predicated on MPP, which controls IBC switching processes for controlled DC output voltage. Figure 1 depicts the structure of the proposed hybrid power scheme.

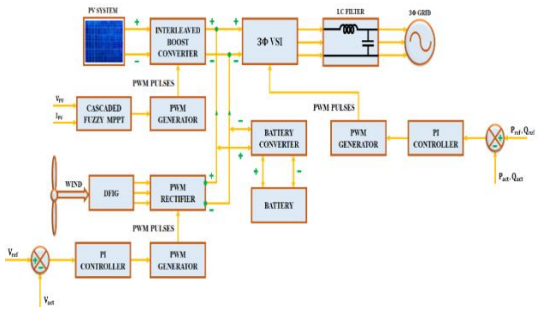

Figure 1. Proposed Hybrid Wind-PV-Battery based microgrid

The AC output voltage obtained from the DFIG based WECS is converted into DC voltage by using a PWM rectifier. The actual voltage of rectifier V_{act} and reference voltage V_{ref} are related and error is created. This error is fed into the PI controller, where efficient error minimization occurs, culminating in the development of a control signal. When this control signal is provided to PWM generator, it produces PWM pulses, that controls switching operations of rectifier thereby generating controlled DC output voltage. The battery which acts as a secondary power source, stores excess power obtained from both PV and WECS. The controlled DC output obtained from both renewable energy sources are converted into AC by using a 3φ VSI. The output voltage obtained from inverter is supplied to 3φ grid via an LC filter as it attenuates harmonics.

3. Proposed System Modelling

3.1. PV Cell Modelling

A single diode model or one diode model is used to derive the basic structure of photovoltaic cell. As shown in Fig.2, an equivalent circuit of a PV system comprises of a diode, photocurrent source, series resistor, and parallel resistor. Based on Shockley diode equation, the value of I_D is given as,

$$I_D = I_0 \left[exp\left(\frac{V_D}{nV_T}\right) - 1 \right] \quad (1)$$

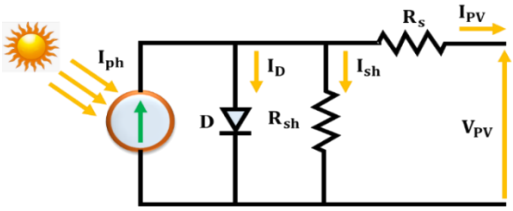

Figure 2. PV cell equivalent circuit model

Where, reverse bias saturation current is specified as I_0, diode current is specified as I_D, Ideality factor of diode is specified as n, thermal voltage is specified as V_T and the voltage across the diode is specified as V_D. The value of thermal voltage is given as,

$$V_T = \frac{kT}{q} \quad (2)$$

Where the electron charge is specified as q, the operating temperature of the cell is specified as T and the Boltzmann constant is specified as k. The I-V characteristics of photovoltaic cell is specified as,

$$I_{PV} = I_{ph} - I_0 \left[exp\left(\frac{V_{PV}+I_{PV}R_S}{nV_T}\right) - 1 \right] - \left(\frac{V_{PV}+I_{PV}R_S}{R_P}\right) \quad (3)$$

Where, the terms I_{ph} and I_{PV} refers to the light-generated and terminal current respectively. The terms R_P and R_s is used to represent the parallel and series resistance respectively. The influence of temperature on photo-generated current is given as,

$$I_{ph} = I_{pvn} + K_I \Delta T \quad (4)$$

In nominal condition, the light generated current is specified as I_{pvn} and the terms ΔT and K_I is used to specify the temperature difference and the ratio of short circuit current to temperature respectively.

3.2. Interleaved Boost Converter

The converter circuit is simple in design with excellent current sharing features, low input current ripple and no reverse recovery loss. The inductors L_1 and L_2 have the same winding orientation and are closely coupled. Figure 3 depicts the IBC basic circuit schematic and comparable circuit diagram. Six modes of operation of IBC is explained in Fig. 4.

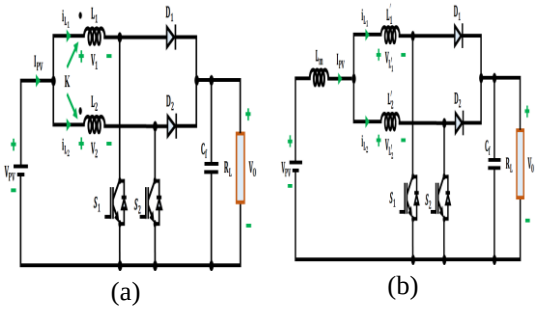

Figure 3. IBC (a) Circuit diagram and (b) Equivalent circuit diagram

The following equations describe how the inductors are related:

$$L_1' = L_1 - L_m \quad (5)$$

$$L_2' = L_2 - L_m \quad (6)$$

$$L_m = k\sqrt{L_1 L_2} \quad (7)$$

Here, k - coupling coefficient,

L_1', L_2' - the leakage inductances of two inductors in equivalent circuit and

L_m- mutual inductance.

Mode a

When power switch S_1 is ON at timet_o, the current i_{L_1} increases and inductor L'_2 discharges the stored energy, which is acquired from previous switching cycle. A rate of change of current i_{L_2} is calculated as follows:

$$\frac{di_{L_2}}{dt} = \frac{-V_o}{L'_1+L'_2} \tag{8}$$

Mode b

During the interval $(t_1 - t_2)$, power switches S_1 and S_2 are turned ON and OFF, respectively. The current i_{L_2} value reaches zero and the current i_{L_1} keeps on increasing at time t_1. At this stage, both the diodes D_1 and D_2 are reverse biased and the rate of change of current i_{L_1} is calculated as follows:

$$\frac{di_{L_1}}{dt} = \frac{V_{PV}}{L_1} \tag{9}$$

Here, $L_1 = L'_1 + L_m$

Mode c

During the interval $(t_2 - t_3)$, both the switches S_1 and S_2 are in OFF condition. Meanwhile, the diode D_2 does not conduct and the diode D_1 is forward biased. Energy stored in inductor L'_1 discharges and flows to load through D_1.

$$\frac{di_{L_1}}{dt} = \frac{-(V_o - V_{PV})}{L_1} \tag{10}$$

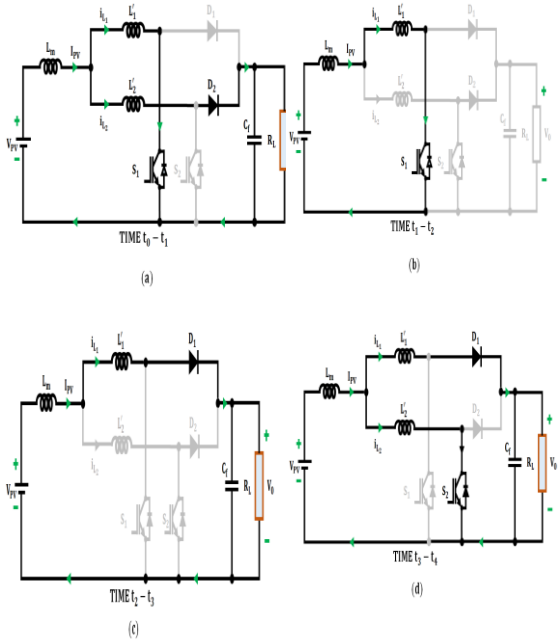

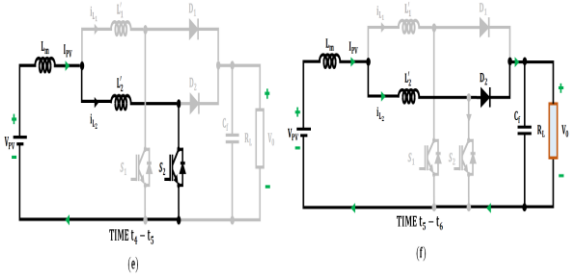

Figure 4. Operating modes of IBC

Mode d

During the interval $(t_3 - t_4)$, power switches S_1 and S_2 are turned OFF and ON, respectively. The current i_{L_2} increases and the diode D_1 operates in forward biased, while diode D_2 operates in reverse biased condition. The inductor L'_1 gets discharged and rate of change of current flowing through inductor L'_1 is given as,

$$\frac{di_{L_1}}{dt} = \frac{-V_o}{L'_1+L'_2} \tag{11}$$

Mode e

During the interval $(t_4 - t_5)$, the switch S_1 is turned OFF, while S_2 is turned OFF. Both the diodes D_1 and D_2 are reverse biased and the current flowing through inductor L'_2 increases at a rate of

$$\frac{di_{L_2}}{dt} = \frac{V_{PV}}{L_2} \tag{12}$$

Here, $L_2 = L'_2 + L_m$

Mode f

During the interval $(t_5 - t_6)$, both the switches S_1 and S_2 are in OFF condition. At this stage, the diode D_1 does not conduct and the inductor L'_2 gets discharged. The rate of change of current i_{L_2} is calculated as follows:

$$\frac{di_{L_2}}{dt} = \frac{-(V_o - V_{PV})}{L_2} \tag{13}$$

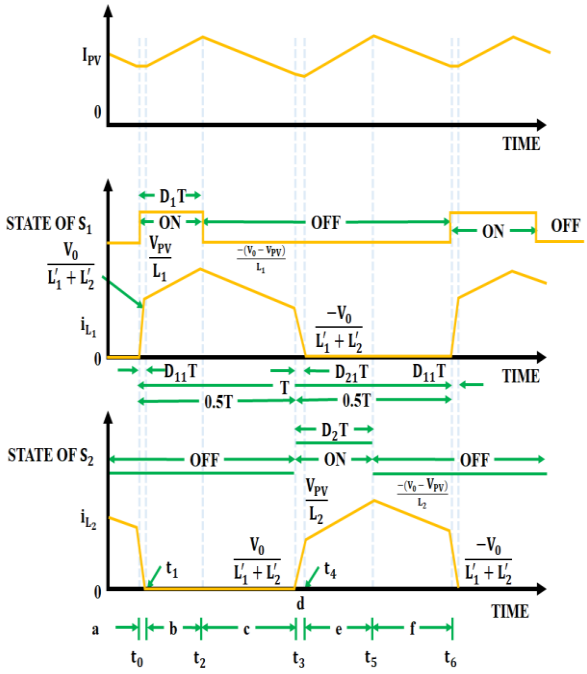

Figure 5. Current waveforms of IBC

The current waveforms of IBC is shown in Fig. 5. Through an effective operation of IBC in conjunction with the CFLC based MPPT, the drawback associated with varying operating condition is overcome and maximum power is transferred to the grid.

3.3. Cascaded Fuzzy Logic Controller (Cflc) Mppt

A CFLC based MPPT is used to facilitate the IBC to enable maximal power transference. Cascaded control technique ensures overall system control in addition to potential of providing speedier responses to compensate for disruptions. Two FLCs are coupled in series combination to form a CFLC, where the output signal obtained from first FLC is provided as input to the second FLC. Since fuzzy sets are incredibly beneficial at tackling the problem of intermittency and uncertainty in a system, fuzzy cascade control structure are designed and employed in this applications. Fig. 6. illustrates the structure of CFLC based MPPT approach. The drawbacks that are associated with traditional MPPT methods such as steady state error, relaxing time and rapid fluctuations around MPP are overcome using CFLC.

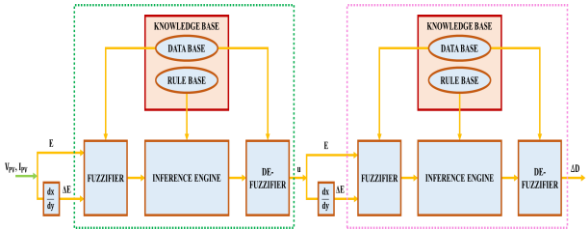

Figure 6. Structure of CFLC based MPPT

The continuous transformation of the input analogue signals to digital quantities is carried out using the FLC. The FLC functions at a higher power effectiveness than other conventional MPPT techniques whenever there is a sudden change in the load current or irradiance.

$$\frac{dP_{PV}}{dV_{PV}} = E = \frac{P_{PV}(k)-P_{PV}(k-1)}{V_{PV}(k)-V_{PV}(k-1)} \quad (14)$$

$$\Delta\frac{dP_{PV}}{dV_{PV}} = \Delta E = E(k) - E(k-1) \quad (15)$$

Where, the terms V_{PV} and P_{PV} is utilized to represent PV panel output voltage and power respectively and sampling time is specified by the term n. The terms E and ΔE is used to represent error and rate of change in error respectively. The output from CFLC is used to alter the duty cycle of the IBC to allow utmost possible power to the grid from the solar panel. The vital components of FLC are,

- **Fuzzifier:** In order to activate the rules, the input fuzzy sets are generated by conversion of crisp values.
- **Rule base:** The operation of the controller are defined by using a set of IF-THEN statements.
- **Inference engine:** Through the application of the rules, the output fuzzy sets are obtained by the transformation of input fuzzy sets.
- **Defuzzifier:** The crisp values are obtained by the conversion of output fuzzy sets.

The change in power and voltage are represented using the terms ΔP and ΔV respectively. The FLC when adopted for MPPT operation, operates based on the following rules:

- D is increased by –ΔD, if $\Delta V < 0$ and $\Delta P < 0, \Delta P/\Delta V > 0$.
- D is increased by +ΔD, if $\Delta V < 0$ and $\Delta P > 0, \Delta P/\Delta V < 0$.
- D is decreased by –ΔD, if $\Delta V > 0$ and $\Delta P > 0, \Delta P/\Delta V > 0$.
- D is decreased by +ΔD, if $\Delta V > 0$ and $\Delta P < 0, \Delta P/\Delta V < 0$.
- MPP is accomplished, if $\Delta P = 0$.

Since, $E = \Delta P/\Delta V$, it can be concluded that D=D+Δ if $E < 0$, D=D-ΔD if $E > 0$ and D=D if E=0. Using membership functions, the fuzzy linguistic variables are created by the conversion of crisp values in the fuzzification stage. In this MPPT technique, five fuzzy sets are includes, in which Negative Big is specified as (NB), Positive Small as (PS), Negative Small as (NS), Positive Big as (PB) and Zero is specified as (Z) in addition to triangular membership functions are chosen. Table 1 presents the fuzzy rules for the proposed MPPT technique. The membership functions of fuzzy are displayed in Fig. 7.

Table 1: Fuzzy rules for the proposed MPPT

$E/\Delta E$	NB	NS	ZE	PS	PB
NB	ZE	ZE	PB	PB	PB
NS	ZE	ZE	PS	PS	PS
ZE	PS	ZE	ZE	ZE	NS
PS	NS	NS	NS	ZE	ZE
PB	NB	NB	NB	ZE	ZE

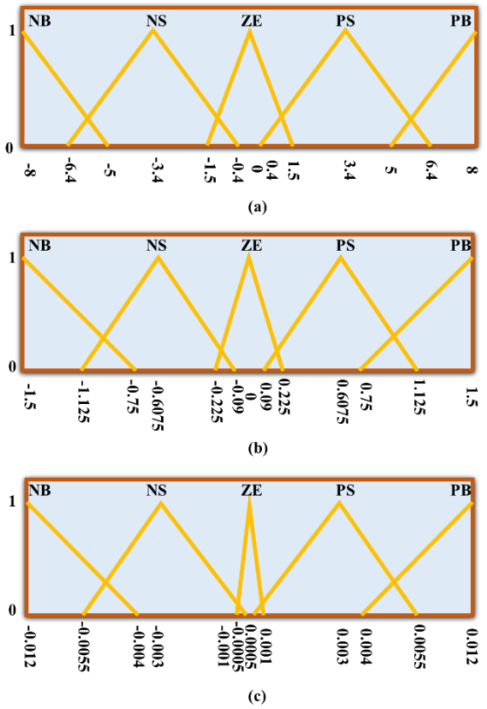

Figure 7. (a) Membership function of E ,ΔE and output duty cycle.

The accuracy and speed of the FLC is highly influenced by the membership functions. The proposed CFLC based MPPT technique has excellent dynamic performance. The output ΔD of the CFLC is provided to the PWM generator and the pulses produced by the PWM generator is used to control the working of IBC.

3.4. Modelling of DFIG Based WECS

Wind turbine hitches the driving energy of wind to generate mechanical energy, which in turn is transformed to electrical energy by the application of DFIG. The wind turbine characteristics are described using the following equations.

$$T_m = \frac{0.5\rho\pi R^2 C_p(\lambda,\beta)V_{wind}^3}{\omega_{WT}} \quad (16)$$

$$C_p(\lambda,\beta) = 0.645\left(\frac{116}{\lambda_i} - 0.4\beta - 5\right)e^{-21/\lambda_i} \quad (17)$$

$$\lambda_i = \frac{1}{1/\lambda + 0.08\beta - 0.035/(\beta^3+1)} \quad (18)$$

Where the term ρ specifies air density, β specifies pith angle, λ specifies the tip speed ratio, C_p specifies power coefficient and R specifies blade radius. The DFIG is a high-efficiency AC asynchronous variable-speed generator with improved reactive power controllability, reduced mechanical stress, and improved energy harvesting capability. Fig.8. presents the equivalent circuit of DFIG in a dq frame.

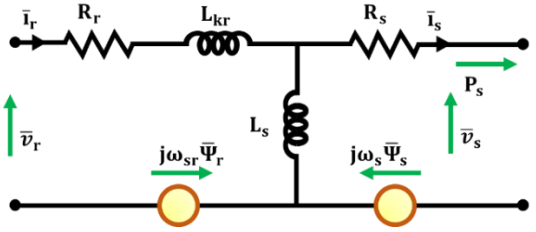

Figure 8. DFIG equivalent circuit

The modelling of DFIG is obtained using the following equations.

$$\bar{v_s} = -R_s\bar{i_s} + \frac{1}{\omega_b}\frac{d\bar{\Psi_s}}{dt} + j\frac{1}{\omega_b}\frac{d\theta_s}{dt}\bar{\Psi_s} \quad (19)$$

$$\bar{v_r} = -R_r\bar{i_r} + \frac{1}{\omega_b}\frac{d\bar{\Psi_r}}{dt} + j\frac{1}{\omega_b}\frac{d\theta_r}{dt}\bar{\Psi_r} \quad (20)$$

$$\bar{\Psi_s} = L_s(-\bar{i_s} + \bar{i_r}), \bar{\Psi_r} = \bar{\Psi_s} + L_{kr}\bar{i_r} \quad (21)$$

$$t_e = -Im\left(\bar{\Psi_s}\underline{i_r}\right), p_s = -Re(\bar{v_s}\underline{i_s}) \quad (22)$$

Where, stator and rotor voltages are specified as v_s and v_r and current as i_s and i_r respectively, the stator and rotor resistance is expressed as R_s and R_r , inductance are specified as L_s and L_r and flux is represented as Ψ_s and Ψ_r respectively and the term t_e is used to represent the positive torque. The AC output generated by the DFIG is transformed

effectively to DC by the implementation of PWM rectifier. The actual voltage of rectifier V_{act} and reference voltage V_{ref} are evaluated. The error produced is supplied to PI controller for achieving error compensation. The output from PI controller assists PWM generator in generating PWM pulses, which regulates switching operation of rectifier to acquire a stable DC voltage as output.

3.5. Battery Energy Storage System (Bess)

The ESS mainly composed of battery and a battery converter that are linked to DC-link of hybrid renewable energy based microgrid as shown in Fig. 9. The main function of battery converter is to keep DC link voltage stable irrespective of power variations in source. Two PI controllers are connected in series for the purpose of maintaining DC link voltage.

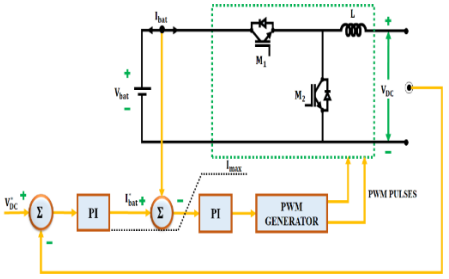

Figure 9. Structure of BESS with battery converter

One PI controller performs voltage error compensation, whereas the other PI controller performs current error compensation. The SOC of a battery is expressed by the following equation as,

$$SOC = 100\left[1 + \frac{\int I_{bat} dt}{Q}\right] \tag{23}$$

Here, Q refers to battery capacity and battery charging current is represented by I_{bat}. A battery's charging and draining behaviour is determined by elements such as power capacity, SOC, and demand. The battery's energy constraints are ascertained by the SOC limits, which is given below,

$$SOC_{min} \leq SOC \leq SOC_{max} \tag{24}$$

Here, SOC_{max} and SOC_{min} are the maximum and minimum allowable states for the battery safety, respectively.

3.6. Grid Voltage Synchronization Using Synchronous Reference Frame Control

Grid voltage and current signals are transformed by a reference frame transformation module in SRF or dq control into a reference frame that rotates in sync with the grid voltage. i.e., abc → dq. As a result of this process, control variables are changed into dc quantities so that filter and control actions are accomplished more easily. The operation of grid tied inverter is controlled by using two PI controllers as illustrated in the Fig. 10. A PI controller is a current control technique that regulates the DC variables in an effective manner and it is implemented in dq frame in this work. The actual direct axis current I_d and reference direct axis current I_d^* are contrasted and an error signal is formed, which is provided as input to PI controllers. Likewise, actual quadrature axis current I_q and reference quadrature axis current I_q^* are analyzed and an error signal produced is provided as input to other PI controller. An errors are completely minimized by proportional and integral process that take place inside PI controllers.

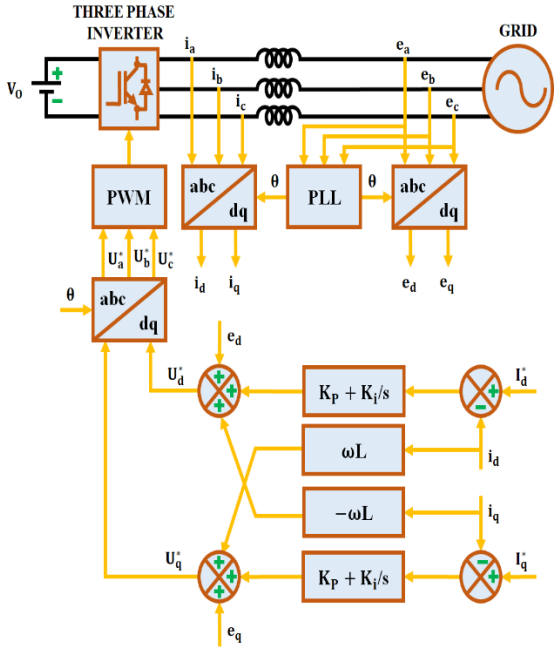

Figure 10. Asynchronous PI controller based Grid voltage synchronization

The general output equation of PI controller is specified as,

$$u(t) = K_P . e(t) + K_I \int e(t) . dt \tag{25}$$

Here, K_P → proportional gain, K_I → integral gain and $e(t)$ → error signal

The output voltage of grid tied inverter, which is specified in synchronous (dq) reference frame is written as,

$$\begin{bmatrix} u_d \\ u_q \end{bmatrix} = L\frac{d}{dt}\begin{bmatrix} i_d \\ i_q \end{bmatrix} + R\begin{bmatrix} i_d \\ i_q \end{bmatrix} + \omega L\begin{bmatrix} -i_q \\ i_d \end{bmatrix} + \begin{bmatrix} e_d \\ e_q \end{bmatrix} \quad (26)$$

In the above equation, angular frequency of grid is specified as ω, inductance between 3Ø inverter and grid is L, the terms e_d and e_q represent park transformation components of grid voltage, the terms u_d and u_q represent park transformation components of inverter output and the resistance between three phase inverter and grid is R.

4. Results and Discussion

This research work aims at the development of an effective control approach for the enhancement of power quality of a hybrid power system based microgrid that includes Wind-PV-Battery. The regulation of the PV module output voltage is carried out using IBC and the capturing of maximum power from PV is established using MPPT technique of CFLC. The PI controller based control approach is used for stabilizing the output from WECS. Based on MATLAB simulations, the performance of the developed control approach for the hybrid power system is verified. Table 2 displays the specifications for the parameters of WECS, IBC, PV panel, load in addition to BESS.

Table 2: Parameter Specifications

PV Panel	
Parameters	Ratings
Peak power	7.5 kW
No. of solar PV panels	750 W, 10 $panels$
Short circuit current I_{SC}	62.5 A
Open circuit voltage V_{OC}	22.6 V
Short circuit voltage V_{SC}	12 V
No .of series connected solar cells	36
WECS	
No. of Wind turbines	1
Power	10 kW
Voltage	575 V
Speed range	4 m/s – 16 m/s
INTERLEAVED BOOST CONVERTER	
L_1, L_2	7 mH
C_b	1000 μF
Switching frequency	10 kHz
BESS	
Capacity	100 Ah
No. of battery units	5, 12 V
BATTERY CONVERTER	
L	1 mH
C	1000 μF
Switching frequency	10 kHz
LOAD	
Capacity	5 kW

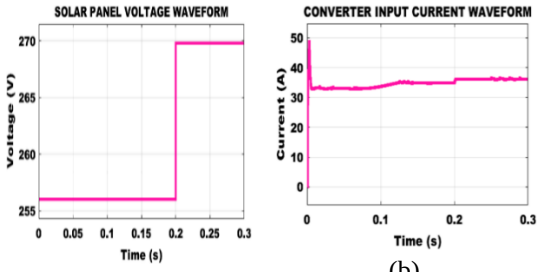

(a) (b)

Figure 11. waveforms representing (a) PV panel voltage (b) Converter input current

The PV is a variable source of power since its output is not constant and is affected by phenomena such as shading, cloud formation, temperature, and meteorological conditions. The PV voltage waveform seen in Fig. 11(a) displays a sudden increase in 0.2s from 256V to 270V owing to the variations in operating conditions. Similarly, the influence of operating condition fluctuation also have a significant impact on the PV panel output current. The output current from PV is provided as input to IBC. The waveforms that depict the converter input current is not stable and it is affected by numerous distortions as depicted in Fig. 11(b). The converter input current is 33A till 0.1s, then it increases to 38A from 0.2s.

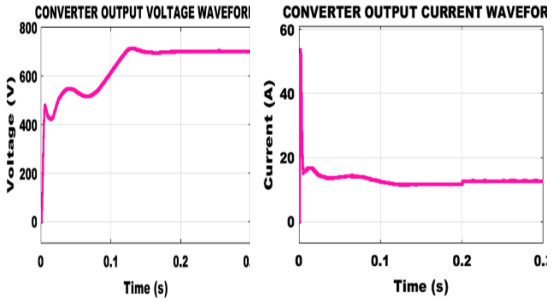

(a) (b)

Figure 12. Output IBC Waveform (a) voltage and (b) current

The waveform that indicates output voltage obtained from IBC is shown in Fig.12. The converter output gradually increases and a magnitude of 700V is obtained at 0.15s. With the assistance of CFLC based MPPT technique, maximum power is captured from the solar panel. The output current of the converter takes 0.15s to stabilize at a value of 16A. At 0.2s, the converter output current increases to 17A with the increase in solar panel output voltage.

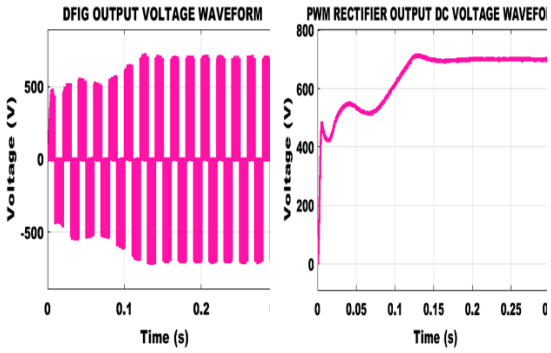

(a) (b)

Figure 13. (a) DFIG output voltage waveform (b) PWM rectifier output voltage waveform

The wind energy is also a variable source of power like the solar energy, so an effective control approach is vital in obtaining a stabilized output from the WECS. The output from DFIG based WECS is indicated in the waveform depicted in Fig .13(a). A stable output voltage of 750V is obtained at 0.15s from the DFIG. The output obtained from the DFIG based WECS is AC in nature, which is converted to DC using the PWM rectifier. The output voltage from PWM rectifier as illustrated in Fig. 13 (b) is free from peak overshoot conditions and it gives a constant voltage of 700V from 0.15s. Thus, the adopted control approach centred on PI controller is effective in stabilizing the DC output from the DFIG based WECS.

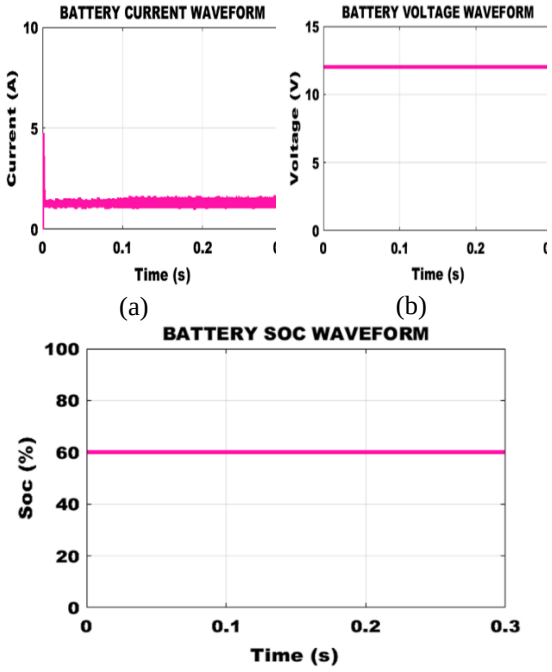

(a) (b)

(c)

Figure 14. Battery (a) Current waveform (b) Voltage waveform and (c) SOC waveform

The battery current waveform is seen in Fig. 14 (a) from which, magnitude of current from battery is 1A is observed. The battery voltage waveform is displayed in Fig. 14 (b) shows stable voltage of 12V is maintained. SOC, which is the amount of charge available in battery with respect to its capacity is a vital component required for the management of BESS. The SOC of the battery is 60% as seen in Fig.14 (c) and based on the value of battery SOC, the charging and discharging process takes place.

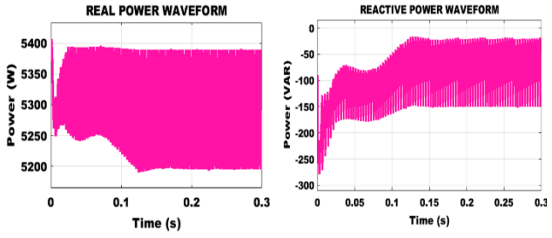

(a) (b)

Figure 15. (a) Real power waveform and (b) Reactive power waveform

Fig. 15 depicts real and reactive power waveform. A value of real power is constantly varied between values of 5380W and 5180 from 0.14s. The value of reactive power is very low and it constantly varies between the values of -25VAR to -170VAR from 0.15s.

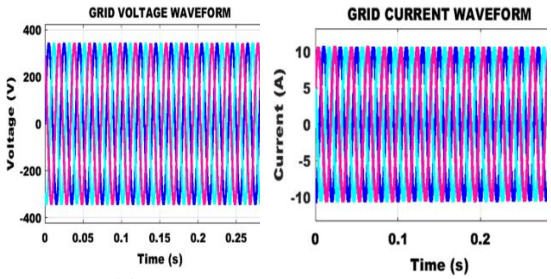

(a) (b)

Figure 16. Waveform for Grid (a) voltage (b) current

The PI controller with the assistance of dq theory, aids in effective grid synchronization and a stable voltage and current is obtained without fluctuations. The waveforms that represent grid current and voltage is shown in Fig. 16. A grid voltage of 230V and grid current of 10A is obtained using this control approach.

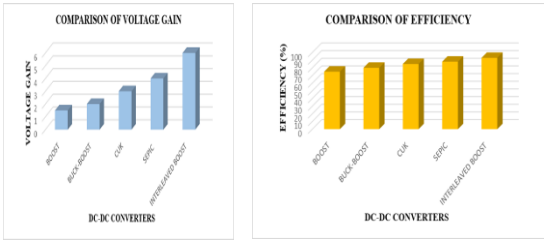

(a) (b)

Figure 17. DC-DC converter Comparison of (a) Voltage gain and (b) Efficiency

The effectiveness of IBC in enhancing operation of photovoltaic system is ascertained by comparing its efficiency and voltage gain with several other available converters as seen in Fig. 17. The IBC has an outstanding efficiency of 93% in addition to a better voltage gain of 1:6. Thereby the adopted control approach for the hybrid power system displays superior performance in curtailing power quality issues and enhancing the stability of microgrid.

5. Conclusion

The purpose of this article is to design an effective control strategy for improving power quality of hybrid power system based microgrid that includes Wind-PV-Battery. The booming expansion of PV and WECS based power production has been necessitated due to the ever-increasing demand for power, as well as the need to develop decarbonized power generation system to address climate change. The introduction of BESS eliminates the intermittency and uncertainty associated with PV and WECS. The conversion of output voltage from PV to a desired level is carried out using IBC with an excellent efficiency of 93% and maximum power is extracted from PV using CFLC- MPPT technique. The DFIG based WECS has wide speed operational range in addition to enhanced power capture capability. The AC to DC conversion of the output from WECS is carried out using PWM rectifier, which is controlled using PI controller. The SOC of BESS is managed using the application of PI controller and effective grid voltage synchronization is achieved using dq theory. From the simulation results obtained from MATLAB, performance of proposed control approach in maintaining power quality and strength of microgrid is verified.

References

[1] A. Merabet, K. Tawfique Ahmed, H. Ibrahim, R. Beguenane and A. M. Y. M. Ghias, "Energy Management and Control System for Laboratory Scale Microgrid Based Wind-PV-Battery," in *IEEE Transactions on Sustainable Energy*, Vol. 8, No. 1, pp. 145–154, 2017.

[2] M. Nurunnabi, N. K. Roy, E. Hossain and H. R. Pota, "Size Optimization and Sensitivity Analysis of Hybrid Wind/PV Micro-Grids- A Case Study for Bangladesh," in *IEEE Access*, Vol. 7, pp. 150120–150140, 2019.

[3] M. N. Musarrat and A. Fekih, "A Fault-Tolerant Control Framework for DFIG-Based Wind Energy Conversion Systems in a Hybrid Wind/PV Microgrid," in *IEEE Journal of Emerging and Selected Topics in Power Electronics*, Vol. 9, No. 6, pp. 7237–7252, 2021.

[4] B. Mangu, S. Akshatha, D. Suryanarayana and B. G. Fernandes, "Grid-Connected PV-Wind-Battery-Based Multi-Input Transformer-Coupled Bidirectional DC-DC Converter for Household Applications," in *IEEE Journal of Emerging and Selected Topics in Power Electronics*, Vol. 4, No. 3, pp. 1086–1095, 2016.

[5] N. M. C. M. and J. P., "Realization of Cascaded H-Bridge Multilevel Inverter Based Grid Integrated Solar Energy System With Band Stop Generalized Integral Control," in IEEE Transactions on Industry Applications, Vol. 57, No. 1, pp. 764–773, 2021.

[6] F. Keyrouz, "Enhanced Bayesian Based MPPT Controller for PV Systems," in IEEE Power and Energy Technology Systems Journal, Vol. 5, No. 1, pp. 11–17, 2018.

[7] R. Errouissi, A. Al-Durra and S. M. Muyeen, "A Robust Continuous-Time MPC of a DC–DC Boost Converter Interfaced With a Grid-Connected Photovoltaic System," in IEEE Journal of Photovoltaics, Vol. 6, No. 6, pp. 1619–1629, 2016.

[8] M. Das, M. Pal and V. Agarwal, "Novel High Gain, High Efficiency DC–DC Converter Suitable for Solar PV Module Integration With Three-Phase Grid Tied Inverters," in IEEE Journal of Photovoltaics, Vol. 9, No. 2, pp. 528–537, 2019.

[9] J. C. d. S. de Morais, J. L. d. S. de Morais and R. Gules, "Photovoltaic AC Module Based on a Cuk Converter With a Switched-Inductor Structure," in IEEE Transactions on Industrial Electronics, Vol. 66, No. 5, pp. 3881–3890, 2019.

[10] K. Nathan, S. Ghosh, Y. Siwakoti and T. Long, "A New DC–DC Converter for Photovoltaic Systems: Coupled-Inductors Combined Cuk-SEPIC Converter," in IEEE Transactions on Energy Conversion, Vol. 34, No. 1, pp. 191–201, 2019.

[11] H. Rezk, M. Aly, M. Al-Dhaifallah and M. Shoyama, "Design and Hardware Implementation of New Adaptive Fuzzy Logic-Based MPPT Control Method for Photovoltaic Applications," in IEEE Access, Vol. 7, pp. 106427–106438, 2019.

[12] K. Y. Yap, C. R. Sarimuthu and J. M. -Y. Lim, "Artificial Intelligence Based MPPT Techniques for Solar Power System: A review," in Journal of Modern Power Systems and Clean Energy, Vol. 8, No. 6, pp. 1043–1059, 2020.

[13] J. Ahmed and Z. Salam, "An Enhanced Adaptive P&O MPPT for Fast and Efficient Tracking Under Varying Environmental Conditions," in IEEE Transactions on Sustainable Energy, Vol. 9, No. 3, pp. 1487–1496, 2018.

[14] M. I. Mosaad, A. Abu-Siada and M. F. El-Naggar, "Application of Superconductors to Improve the Performance of DFIG-Based WECS," in *IEEE Access*, Vol. 7, pp. 103760–103769, 2019.

[15] V. Yaramasu, B. Wu, P. C. Sen, S. Kouro and M. Narimani, "High-power wind energy conversion systems: State-of-the-art and emerging technologies," in Proceedings of the IEEE, Vol. 103, No. 5, pp. 740–788, 2015.

[16] R. H. Byrne, T. A. Nguyen, D. A. Copp, B. R. Chalamala and I. Gyuk, "Energy Management and Optimization Methods for Grid Energy Storage Systems," in *IEEE Access*, Vol. 6, pp. 13231–13260, 2018.